

To be submitted to  
Nuclear Physics A

ISTITUTO NAZIONALE DI FISICA NUCLEARE  
Laboratori Nazionali di Frascati

LNF-78/36(P)  
24 Agosto 1978

F. Balestra, M.P. Bussa, L. Busso, I. V. Falomkin, R. Garfagnini, C. Guaraldo, V.I. Lyashenko, A. Maggiora, F. Nichitiu, G. Piragino, G.B. Pontecorvo, R. Scrimaglio and Yu. A. Shscherbakov: ON THE COLLECTIVE ISOBARIC RESONANCES IN PION-NUCLEUS SCATTERING AT INTERMEDIATE ENERGIES.

F. Balestra<sup>(x)</sup>, M. P. Bussa<sup>(x)</sup>, L. Busso<sup>(x)</sup>, I. V. Falomkin<sup>(o)</sup>, R. Garfagnini<sup>(x)</sup>, C. Guaraldo, V. I. Lyashenko<sup>(o)</sup>, A. Maggiora, F. Nichitiu<sup>(o)(+)</sup>, G. Piragino<sup>(x)</sup>, G. B. Pontecorvo<sup>(o)</sup>, R. Scrimaglio and Yu. A. Shcherbakov<sup>(o)</sup>: ON THE COLLECTIVE ISOBARIC RESONANCES IN PION-NUCLEUS SCATTERING AT INTERMEDIATE ENERGIES. -

ABSTRACT.

The excitation functions of differential cross sections in pion-nucleus scattering at intermediate energies have been obtained by fitting in the c. m. s. with Legendre polynomials all the existing data on  $^1\text{H}$ ,  $^2\text{H}$ ,  $^3\text{He}$ ,  $^4\text{He}$ ,  $^{12}\text{C}$  and  $^{16}\text{O}$ . The spectra have then been deduced calculating the maximum likelihood Lorentz lines through a Monte Carlo method. Among the main features, we find a resonant behaviour of the excitation functions at energies much lower compared to the free  $\Delta$ -resonance position. The shift is angle-dependent and A-dependent. A possible explanation of the downward energy shift is given on the ground of the recent developments of the collective isobaric resonance model.

1. - INTRODUCTION.

The most striking feature in pion-nucleon scattering at intermediate energies is the well known  $\Delta(1232)\text{P}_{33}$  resonance in the total cross section at pion energy  $E = 180$  MeV and with a width  $\Gamma_N \approx 110$  MeV<sup>(1)</sup>.

Excitation functions of differential cross sections at all angles exhibit the same behaviour.

A slight downward energy shift of the resonance occurs in the pion-nucleon case<sup>(2)</sup>. Pion-proton scattering below 300 MeV is almost completely dominated by the  $l=1$  partial wave due to the isospin  $\frac{3}{2}$ , spin  $\frac{3}{2}$  P-wave resonance. At  $E = 195$  MeV, the phase shift for this channel passes very rapidly through  $90^\circ$ . Correspondingly, since this one wave dominates the scattering, the real part of the forward scattering amplitude  $\text{Re} f_{\pi N}(0^\circ) = 0$  at  $E = 195$  MeV. However, because of the momentum factor  $1/k$  in the expression for the imaginary part  $\text{Im} f_{\pi N}(0^\circ)$ , the  $\text{Im} f_{\pi N}(0^\circ)$

---

(x) Istituto di Fisica dell'Università di Torino, and INFN - Sezione di Torino.

(o) Joint Institute for Nuclear Research, Dubna (USSR).

(+) Institutul de Fizica si Inginerie Nucleara, Bucharest (Romania).

has its maximum shifted downwards slightly to  $E \approx 187$  MeV. Since the expression of the optical theorem for the total cross section has an additional  $1/k$  factor in front, the resonance is shifted down further to the experimental value  $E = 180$  MeV.

Measurements of pion-nucleus total cross sections show a peak clearly related to the 3-3 resonance of the pion-nucleon system<sup>(3)</sup>. However, this experimental peak is broadened and shifted approximately 40-50 MeV downwards in energy compared to the peak in  $\sigma(\pi, N)$  ( $E \approx 130-140$  MeV). Theoretical explanations or calculations of this shift appeared in several studies<sup>(4-7)</sup>. The resonance shift seems not to be an exotic effect<sup>(6)</sup>, but it is simply a consequence of the passage of the pion through a dispersive, absorptive medium<sup>(2)</sup>. This multiple scattering tends to diminish the energy variation of the forward  $\pi$ -nucleus scattering amplitude  $f_{\pi-n}(0^\circ)$  and, thus, leads to a broadening. In addition, including nucleon Fermi motion also broadens and lowers the peak slightly. Multiplication of  $\text{Im } f_{\pi-n}(0^\circ)$  by the energy dependent  $1/k$  term, to form the total pion-nucleus cross-section, therefore, leads to a considerably larger shift in the peak position than was found in the corresponding step for the pion-nucleon cross section.

Moreover, shape and position of the peak in pion-nucleus scattering depend on  $A$ , the mass number of the target nucleus. As  $A$  is increased, the peak becomes broader and its maximum moves to a lower energy. Sedlak and Friedman<sup>(8)</sup> have shown that this  $A$ -dependent behaviour originates in geometric and refractive features, rather than in microscopic nuclear dynamics. This results from the blackness of the nucleus to the pion wave in the 3-3 resonance region.

As far as concerns differential cross sections in pion-nucleus scattering, available data on light nuclei give excitation functions with resonant behaviours at energies much lower compared to position of the  $\Delta$  resonance, especially at large angles<sup>(9)</sup>. Positions and widths of the peaks depend on the scattering angle and also on the mass number.

In order to study the excitation functions of differential cross sections, comparing homogeneously data from experiments covering different energy and angular intervals, we have fitted all the existing data on light nuclei such as  $^1\text{H}$ ,  $^2\text{H}$ ,  $^3\text{He}$ ,  $^4\text{He}$ ,  $^{12}\text{C}$ ,  $^{16}\text{O}$ . The main features of the excitation functions have been then deduced and compared to the elementary pion-nucleon scattering. A possible explanation of the downward energy shifts has been given on the ground of the recent collective resonance model of Klingenberg et al.<sup>(10)</sup> and Händel et al.<sup>(11)</sup>.

## 2. - EXCITATION FUNCTIONS OF DIFFERENTIAL CROSS SECTION FOR LIGHT NUCLEI.

Backward angle ( $\pi^\pm$ ,  $^{12}\text{C}$ ) differential elastic cross section in the energy range 23-90 MeV has been measured by the authors<sup>(12)</sup> with a streamer chamber spectrometer<sup>(13)</sup> exposed to the pion beam of the LEALE Laboratory of Frascati. The spectrometer consisted of a self-shunted streamer chamber filled with  $^4\text{He}$  at 1 atm and placed in an electromagnet. In this way the chamber visualized the incident and the scattered pions for events occurred both in the  $^{12}\text{C}$  external target and in the filling gas.

The corresponding excitation function for  $^{12}\text{C}$  is reported in Fig. 1. The solid line is the maximum likelihood Lorentz function obtained with a Monte Carlo calculation. Our lower energy values ( $E < 20$  MeV) are presently under analysis, however, the figure seems to show a resonant behaviour. The peak position is shifted to an energy much lower compared to the position of the  $\Delta$  resonance in pion-nucleon scattering.

Two large angle ( $\pi^\pm$ ,  $^4\text{He}$ ) values ( $150^\circ \pm 10^\circ$  and  $165^\circ \pm 15^\circ$ ) have been measured<sup>(14)</sup> with the streamer chamber with 81 MeV  $\pi^-$  and 33 MeV  $\pi^+$ . In Fig. 2, the corresponding excitation functions have been deduced from these data and large angle elastic data from other experiments<sup>(15)</sup>. The Lorentz lines show a maximum at  $E = 73.5$  MeV at  $\theta = 150^\circ$  and at  $E = 72.6$  MeV at  $\theta = 165^\circ$ .

A similar behaviour can be found for the large angle excitation function in ( $\pi^\pm$ ,  $^2\text{H}$ ) scattering. In Fig. 3 is reported the excitation function of differential cross section at  $155^\circ \pm 5^\circ$  from the experimental data available in literature on pion-deuteron scattering<sup>(16)</sup>. The figure shows a peak again at a much lower energy ( $E = 98.7$  MeV) compared to free  $\Delta$  resonance.

In order to obtain the excitation functions of differential cross section from light nuclei and to compare in an homogeneous way data from different experiments, we have fitted in the c. m. s.

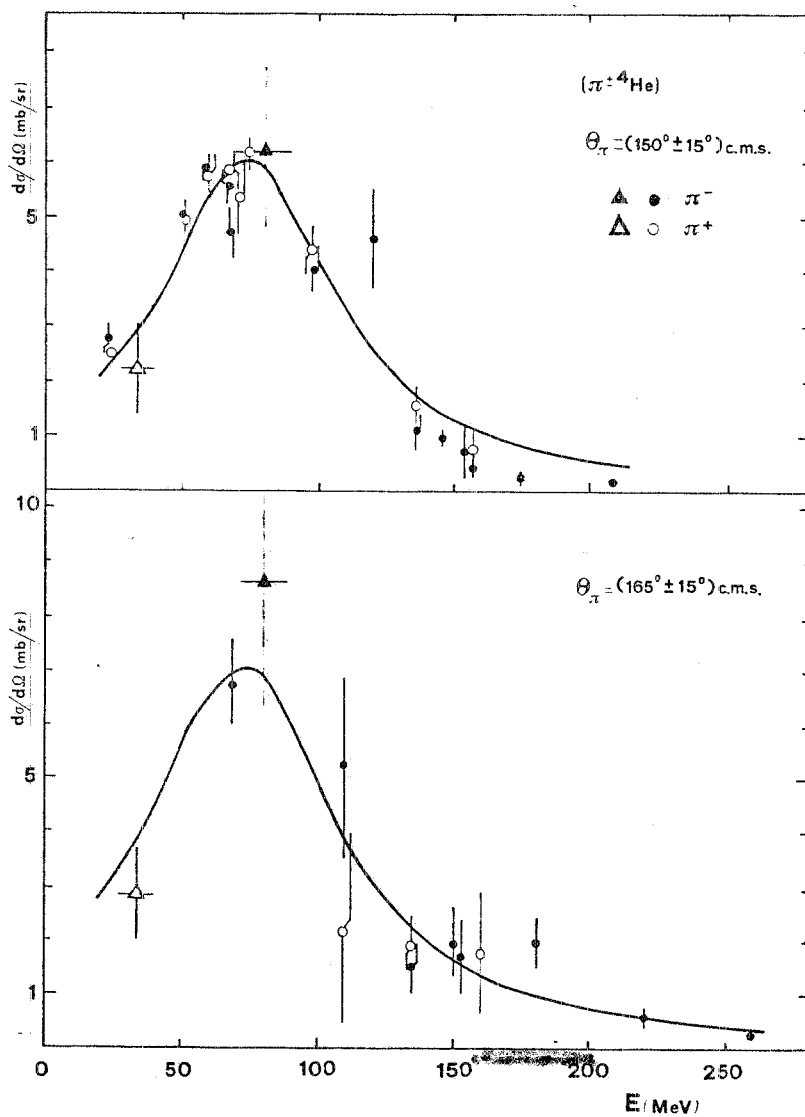
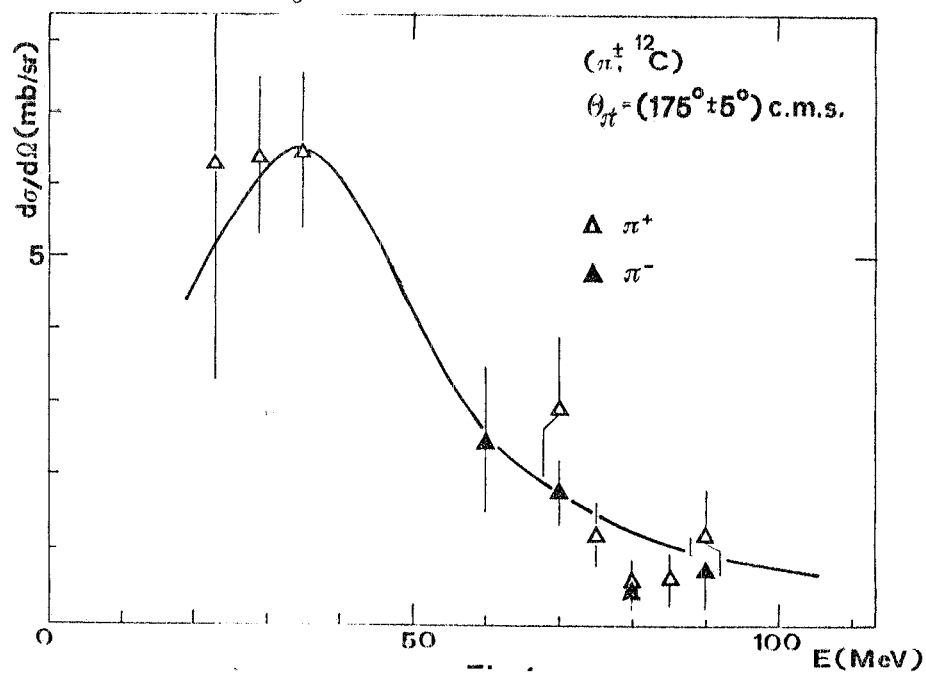


FIG. 1 - Excitation function of  $(\pi^\pm, {}^{12}\text{C})$  differential elastic cross section at  $175^\circ \pm 5^\circ$ . Experimental data: ref. (12). The solid line is the maximum likelihood Lorentz function obtained with a Monte Carlo calculation.

FIG. 2 - Excitation functions of  $(\pi^\pm, {}^4\text{He})$  differential elastic cross sections at  $150^\circ \pm 10^\circ$  and  $165^\circ \pm 15^\circ$ . Experimental data: triangles ref. (14); circles ref. (15). The solid curves are Lorentz lines.

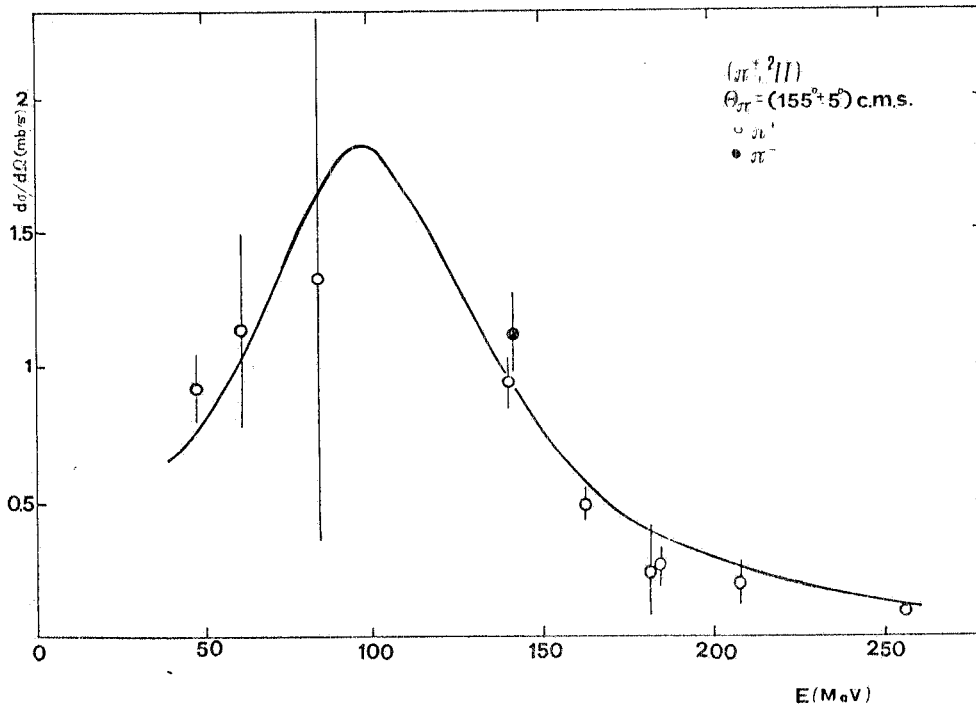


FIG. 3 - Excitation function of  $(\pi^+, {}^2\text{H})$  differential elastic cross section at  $155^\circ \pm 5^\circ$ . Experimental data: ref. (16). The solid curves are Lorentz lines.

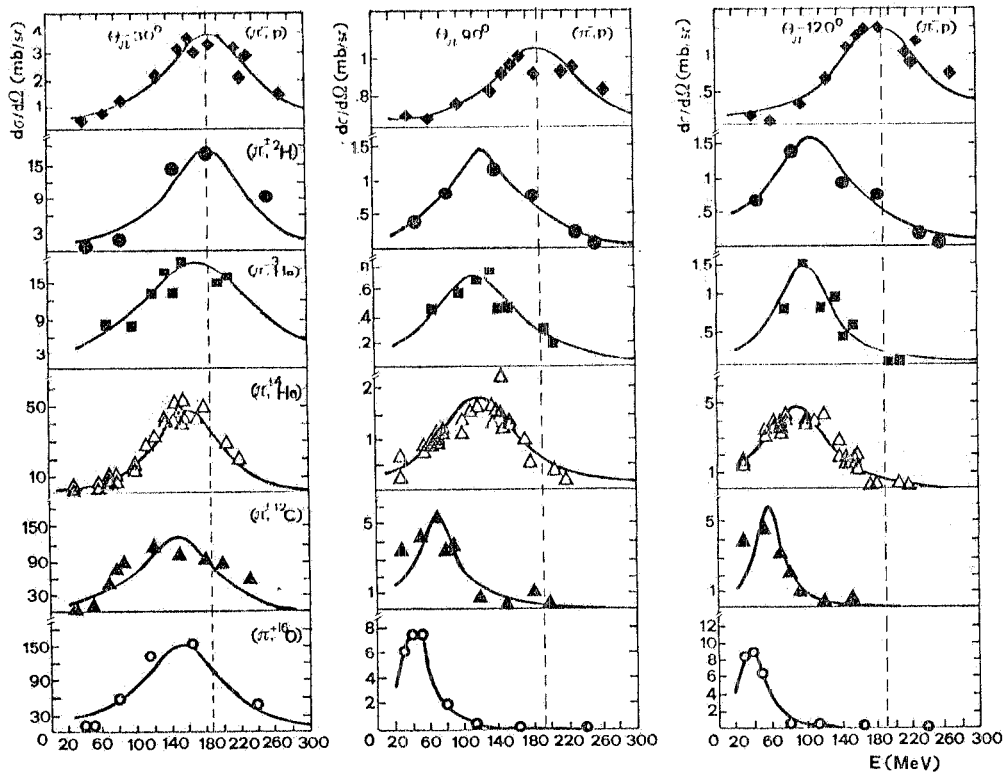


FIG. 4 - Excitation functions of differential elastic cross sections of  $\pi^\pm$  on proton and light nuclei at  $30^\circ$ ,  $90^\circ$  and  $120^\circ$ . Symbols:  $\blacklozenge$  ( $\pi^-, p$ );  $\bullet$  ( $\pi^+, {}^2\text{H}$ );  $\blacksquare$  ( $\pi^-, {}^3\text{He}$ );  $\triangle$  ( $\pi^+, {}^4\text{He}$ );  $\blacktriangle$  ( $\pi^+, {}^{12}\text{C}$ );  $\circ$  ( $\pi^+, {}^{16}\text{O}$ ) represent the best fit value obtained at the energies where differential cross section data are available. The solid curves are Lorentz lines.

with Legendre polynomials all the existing data on  $^1\text{H}$ : ref.(1),  $^2\text{H}$ : ref.(16),  $^3\text{He}$ : ref.(17),  $^4\text{He}$ : ref.(14, 15),  $^{12}\text{C}$ : ref.(12, 18),  $^{16}\text{O}$ : ref.(19). The excitation functions have then been deduced calculating the maximum likelihood Lorentz lines through a Monte Carlo method.

In Fig. 4 the excitation functions of differential cross sections at  $30^\circ$ ,  $90^\circ$  and  $120^\circ$  for light nuclei such as  $^2\text{H}$ ,  $^3\text{H}$ ,  $^4\text{He}$ ,  $^{12}\text{C}$  and  $^{16}\text{O}$  are reported, together with the curves relative to elementary  $\pi^\pm$  scattering.

### 3. - ANALYSIS OF THE EXCITATION FUNCTIONS.

The following main features can be drawn from the analysis of the excitation functions :

- The excitation functions of  $(\pi^\pm, p)$  differential cross sections show a resonant behaviour peaked at the same energy of the free  $\Delta$  resonance over the whole angular interval.
- The excitation functions of  $\pi$ -nucleus differential cross sections show a resonant behaviour peaked at energies much lower compared to the  $\Delta$  position. The shift is angle-dependent and A-dependent: it is as much pronounced as the angle increases and the nucleus is heavier. All this is stressed in Fig. 5, in which are reported the angular dependences of the peak positions for the

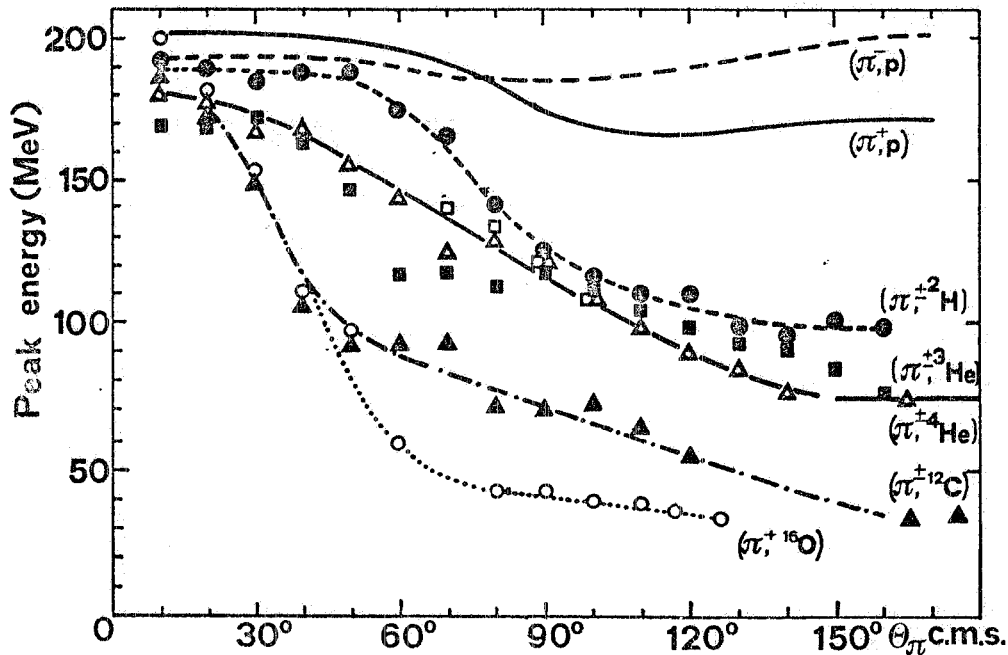


FIG. 5 - Angular behaviours of peak positions of the excitations functions. Solid line :  $(\pi^+, p)$ . Dotted line :  $(\pi^-, p)$  Symbols :  $\bullet$   $(\pi^+, ^2\text{H})$ ;  $\square$   $(\pi^+, ^3\text{He})$ ;  $\blacksquare$   $(\pi^-, ^3\text{He})$ ;  $\Delta$   $(\pi^+, ^4\text{He})$ ;  $\blacktriangle$   $(\pi^+, ^{12}\text{C})$  represent peak positions at  $10^\circ$  intervals, unless the lack of experimental data. Lines are drawn as a guide to eye.

considered nuclei, compared with the behaviours of the elementary processes.  $\Delta$  resonance do not exhibit nearly any angular dependence, as it is known and appears also in the figure. On the contrary, the positions of the peaks of the excitations functions of differential cross sections seem to decrease with the scattering angle, the angular behaviour becoming flat only at backward. Moreover, the angular behaviours of the peak positions show an A-dependence: steeper slopes and lower energy values for heavier nuclei.

What is significant to stress is that, at forward, angular behaviours and peak positions are close to those of the elementary resonances.

- c) The angular behaviours of the momentum transfer  $q_p$  corresponding to the energy value  $E_p$  of the peaks, show (see Fig. 6) the significant feature of the existence, for each nucleus, of some characteristic maximum angle  $\theta_m$  such that, for  $\theta_\pi < \theta_m$  the  $q_p$  values are close to those of  $(\pi^+, p)$ , while for  $\theta_\pi > \theta_m$  the behaviours become nearly flat.

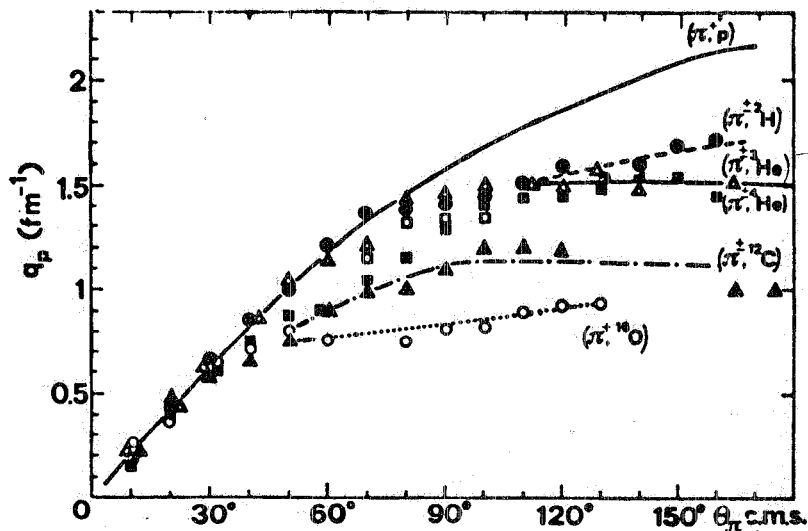


FIG. 6 - Angular behaviours of the momentum transfer  $q_p$  corresponding to the peak positions of the excitation functions. Symbols are those of Fig. 5. Lines are drawn as a guide to eye.

Again, the  $\theta_m$  values are A-dependent: higher for lighter nuclei.

Moreover, the  $\theta_m$  values seem to be close to the first diffraction minima in the differential elastic cross section.

- d) Excitation functions widths at forward angles seem to be almost equal to the  $\Delta$  width value, while at large angle the peaks are as much narrow as heavier is the nucleus.
- e) The ratio between the  $(\pi^+, p)$  differential cross section values corresponding to the excitation function maximum is, in average,  $9.05 \pm 0.1$  over the whole angular interval. This is, as it is known, the  $\Delta^+/\Delta^0$  value and it means that, at the resonance, there is almost no contribution from the  $T = 1/2$  state in  $(\pi^+, p)$  interaction. Moreover, it is a good check of our analysis method.
- f) Peak intensities of the excitation functions of light nuclei at forward angles seem to be Z multiple of the  $(\pi^+, p)$  value. In Table I the light nuclei peak intensities and their ratios  $R_p$  to the  $(\pi^+, p)$  values at  $20^\circ$  are reported. In Fig. 7 the angular distributions of the normalized ratios  $R_p^n = R_p/Z$  are shown. The  $R_p^n(\theta_\pi)$  values range from about unity at forward angles, to about  $0.1 \pm 0.05$  for all the examined nuclei.
- g) The normalized ratios  $R_p^n$ , plotted as a function of  $q_p^2 a^2$ , where  $q_p$  is the momentum transfer corresponding to the peak energy and  $a$  is the equivalent spherical radius of the nucleus show (see Fig. 8) form-factor-like behaviours. It is interesting to note that deuteron behaves differently from all the other light nuclei.

TABLE I - Peak intensities of the excitation functions of light nuclei at  $20^\circ$  and relative ratios  $R_p$  to the  $(\pi^+, p)$  values.

	$(\pi^+, p)$	$(\pi^-, p)$	$(\pi^-, {}^2\text{H})$	$(\pi^-, {}^3\text{He})$	$(\pi^-, {}^4\text{He})$	$(\pi^-, {}^{12}\text{C})$	$(\pi^+, {}^{16}\text{O})$
$(\frac{d\sigma}{d\Omega})_{\text{peak}}(\theta = 20^\circ)$ (mb/sr)	33.87	4.17	33.65	26.30	76.87	275.16	318.87
$R_p$	1	1/8.12	0.99	0.78 <sup>(x)</sup>	2.27	8.12	9.41
$R_p^n \equiv R_p/Z$	1	1/8.12	0.99	0.78 <sup>(o)</sup>	1.13	1.35	1.18

(x) in this case  $R_p$  is defined as the ratio with  $(\pi^-, n) \approx (\pi^+, p)$  cross section.

(o) in this case  $R_p^n \equiv R_p/(A - Z)$ .

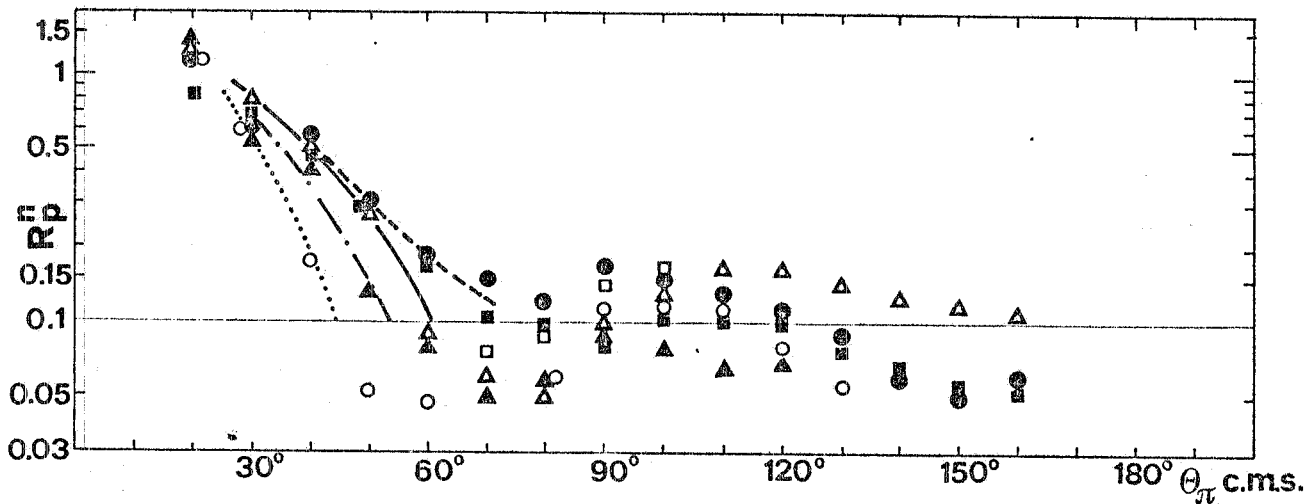


FIG. 7 - Angular behaviours of the Z-normalized ratios  $R_p^n$  between peak intensities of light nuclei excitation functions and  $(\pi^+, p)$  values. Symbols are those of Fig. 5. Lines are drawn as a guide to eye.



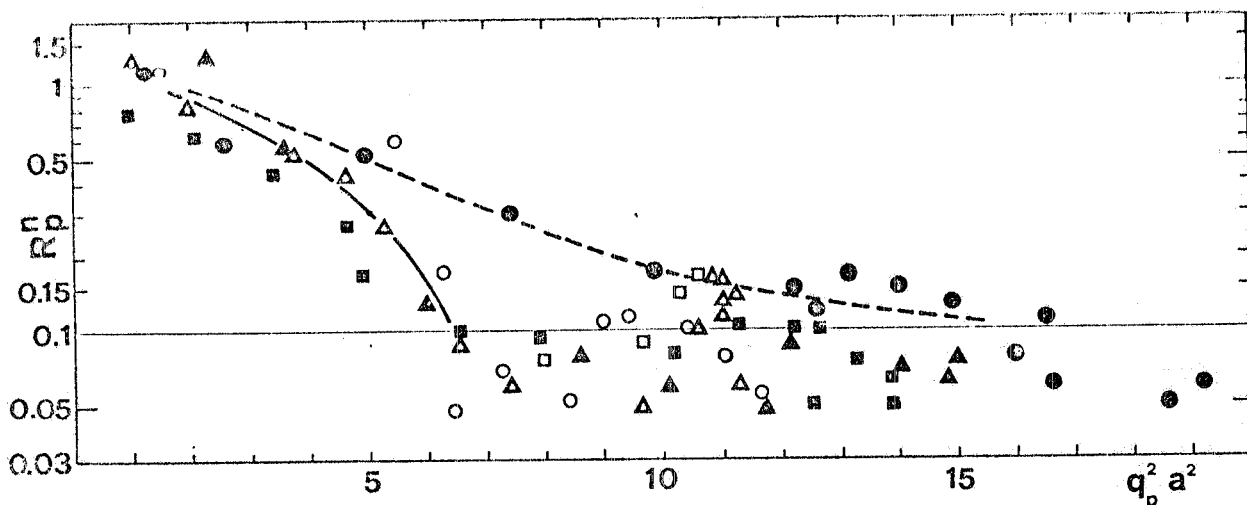


FIG. 8 - Normalized ratios  $R_p^n$  between peak intensities of light nuclei excitation functions and  $(\pi^+, p)$  values, versus  $q_p^2 a^2$ , where  $q_p$  is the momentum transfer corresponding to the peak energy and  $a$  is the equivalent spherical radius of the nucleus. Symbols are those of Fig. 5. Lines are drawn as a guide to eye.

#### 4. - COLLECTIVE RESONANCES IN PION-NUCLEUS SCATTERING.

Explaining the salient features of the above obtained excitation functions of differential cross sections seems to ask for more insight into the dynamics of the elementary processes.

It is well known that pion-nucleon scattering at intermediate energies is dominated by the  $\Delta(1232)$  resonance. From the large elementary cross section  $\pi^+p$  at the resonance energy ( $\sigma \approx 200$  mb) it is to be expected that a conventional multiple scattering approach to pion-nucleus scattering does converge slowly as the corresponding mean free path of such a pion is smaller than average nucleon-nucleon distance in a nucleus. Due to this strong interaction many body effects will appreciably modify the elementary  $\pi$ -nucleon t-matrix, so that the impulse approximation and its modifications are not the adequate description.

A natural way of introducing many body effects is the explicit inclusion of the isobar degrees of freedom of bound nucleons. For such a description of pion-nucleus scattering various more or less closely related models have been developed during the last few years: the Isobar Doorway Model of Kisslinger and Wang<sup>(20)</sup>, the Collective Model of Dillig and Huber<sup>(21)</sup> and the Multiple Scattering Approach of Lenz et al.<sup>(22)</sup>; related aspects have been discussed by Brown and Weise<sup>(23)</sup>.

Following the Collective Model approach, Klingenberg et al.<sup>(10)</sup>, and Händel et al.<sup>(11)</sup> have recently given a new description of pion nucleus scattering, which treats the isobar on the same footing of the nucleon. The model has been applied to elastic and inelastic pion-carbon scattering and to elastic pion-deuteron scattering. The starting point is the assumption that the incoming pion excites a bound nucleon into the  $\Delta$  resonance, thereby creating an isobaric particle-hole ( $\Delta\bar{N}$ ) configuration. Since the  $\Delta$  interacts strongly with the surrounding nucleons, the various ( $\Delta\bar{N}$ ) configurations of the same quantum numbers are coupled, thus leading to new eigenstates  $|A_n^* \rangle$  of the whole nucleus. Those nuclear excitation can decay by emitting a pion, thereby leaving the target nucleus in its ground or one of its excited states, respectively.

The propagator of this system

$$G(\omega) = \left[ H_{\Delta N}(\omega) - \omega \right]^{-1} \quad (1)$$

contains an (energy dependent)  $\Delta N$  interaction,  $V_{\Delta N}$ , and can be expressed by the eigenstates  $|A_n^*\rangle$  of the  $\Delta N$  Hamiltonian as:

$$G(\omega) = \sum_n \frac{|A_n^*\rangle \langle A_n^*|}{\varepsilon_n^{J\pi}(\omega) - \omega} \quad (2)$$

where  $\varepsilon_n^{J\pi}(\omega)$  denotes the complex eigenvalues of the  $A^*$  excitation.

The sum of these  $A^*$  resonances, which differ in their position and width, as well as in their multipolarity and parity, builds up the scattering cross section.

The relevant role of  $V_{\Delta N}$  becomes obvious if one considers the limiting case of no  $\Delta N$  interaction; then the quasi-free scattering amplitude is recovered from eq. (1):

$$\lim_{V_{\Delta N} \rightarrow 0} G(\omega) \rightarrow G_{\text{qf}}(\omega) = [\varepsilon_{\text{free}} - \omega]^{-1} \quad (3)$$

Thus the deviation from quasi free scattering amplitudes reflects the effects of the  $\Delta N$  interaction. In particular, the detailed structure of the  $A^*$  resonances is expected to manifest itself in a sensitive manner at backward angles, where the deviations from the quasi-elastic picture are expected to be more pronounced.

As far as concerns the  $\Delta N$  interaction, since very little is known about it, it has been constructed in a frame of a One Boson Exchange (OBE) model, taking into account explicitly additional contributions resulting from  $\rho$  and  $\omega$  exchange.

The coupling between the various ( $\Delta\bar{N}$ ) configurations is dominantly due to their individual coupling to the pion nucleus continuum channels. In the OBE description, this manifests itself by the fact that the exchanged pion can be a real pion, propagating on its mass shell and therefore leading to a complex and energy dependent  $\Delta N$  interaction.

Summarizing the features of this approach the excitation spectrum of a complex nucleus in the region of the  $\Delta$  resonance is characterized by a number of broad resonances of different multipolarity. Because of the similarity in the description, the occurrence of these  $A^*$  collective resonances can be considered as Giant (3-3) or Giant Isobaric Resonances (GIR).

The significant point, which allows for a connection with the main feature of the experimental excitation spectra of differential cross section, is that an  $A^*$  resonance, whose energy is pushed down below the free (3-3) position, may be the dominant one. This fact results in explicit predictions for the excitation functions of differential cross sections, in the sense that they exhibit drastic different energy behaviours as strong variations in shape and peak position depending on the scattering angle<sup>(10)</sup>.

In Fig. 9 we have reported the excitation functions at some angles for pion-carbon scattering, as resulted from our analysis of the experimental data together with the predictions of the collective resonance model. The qualitative agreement between shapes, widths and positions seems to indicate that the basic ideas about the excitation of isobaric nuclear resonances are realistic.

The less agreement at large angles is possibly an indication that the harmonic oscillator wave functions with the same oscillator parameters for nucleons and the bound isobar, used to diagonalize the  $\Delta N$  Hamiltonian, are only a first-step approximation.

A similar qualitative agreement can be found for the excitation function in pion-deuteron scattering. In Fig. 10 is reported our analysis of the large angle experimental data, together with the collective resonance model prediction, obtained from the angular distributions at various energies calculated by Händel et al.<sup>(11)</sup>. The peak position, far from the free  $\Delta$  resonance, is reproduced.

In the figure is also reported an other excitation curve, peaked at an energy higher than the experimental result. It corresponds to a different choice of the coupling constants  $f_{\rho NN}^2/4\pi$ ,

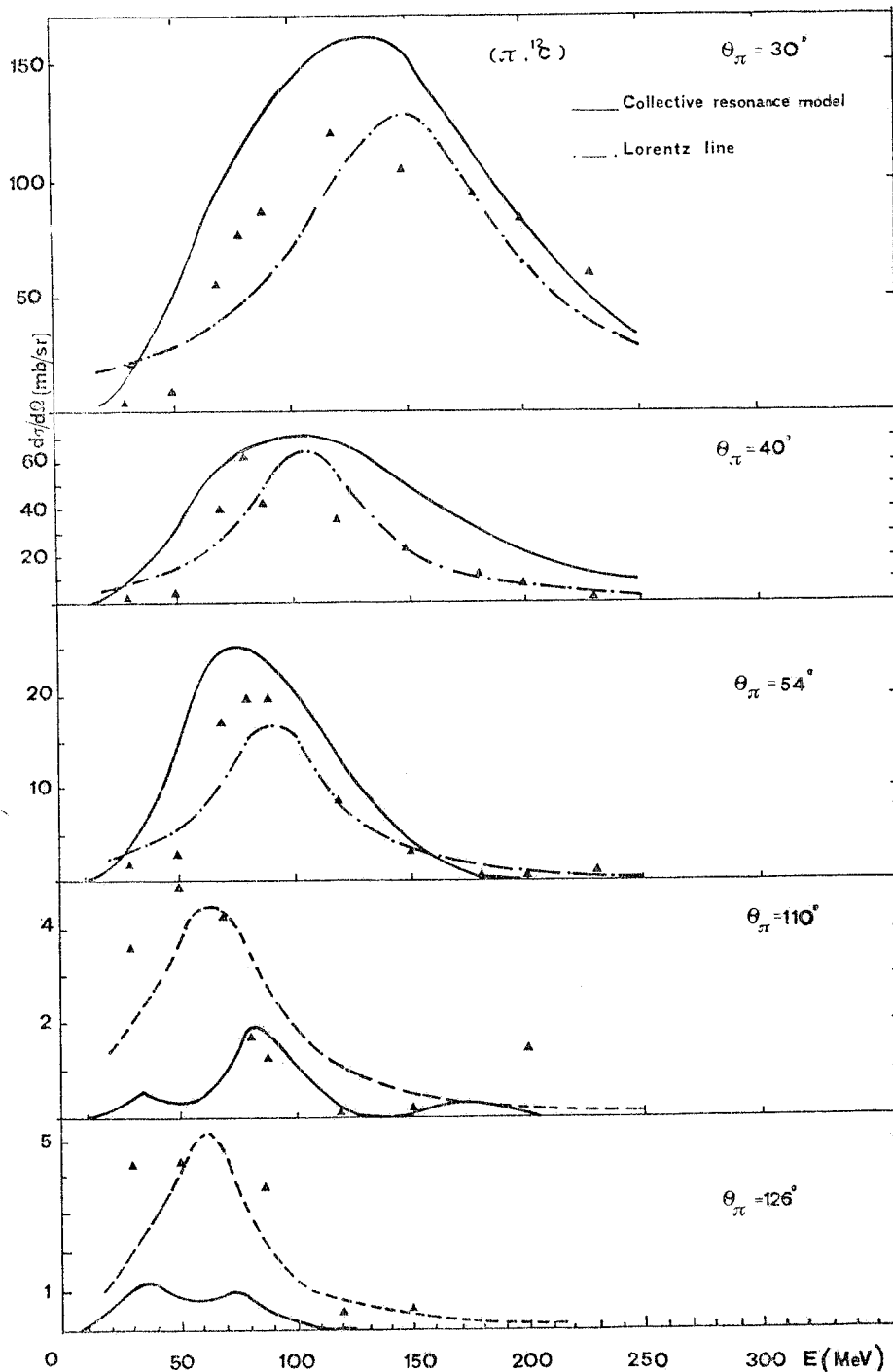


FIG. 9 - Excitations functions of  $(\pi, {}^{12}\text{C})$  differential elastic cross sections. Triangles have the same meaning as in Fig. 4. The solid line represent the prediction of the Collective Resonance Model<sup>(10)</sup>. The dot-dashed curves are Lorentz lines.

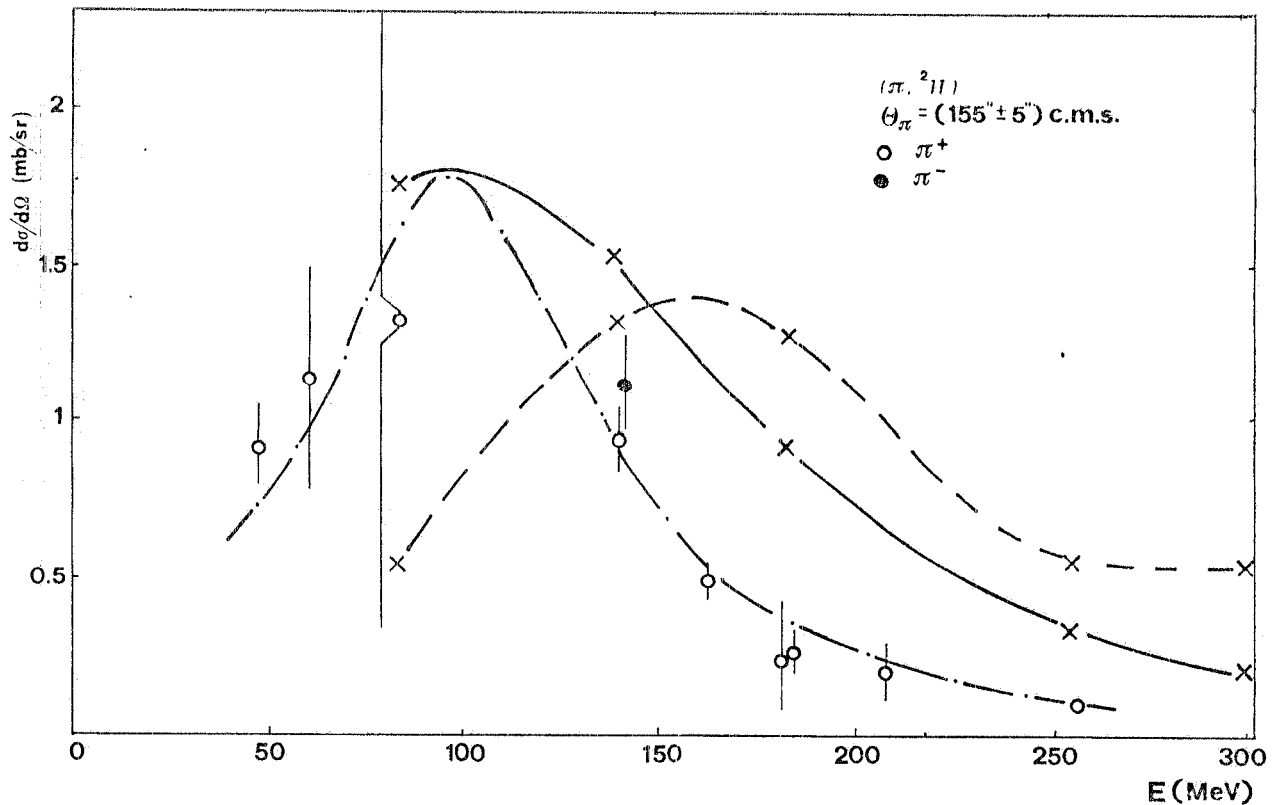


FIG. 10 - Excitation functions of  $(\pi, {}^2\text{H})$  differential elastic cross sections at  $\theta_\pi = 155^\circ \pm 5^\circ$ . Experimental data: ref. (16). The solid and the dashed lines represent the predictions of the Collective Resonance Model obtained for different  $\Delta\text{N}$  interaction parameters<sup>(11)</sup>. The dot-dashed curve is a Lorentz line.

$f_{0\Delta\text{N}}^2/4\pi$ ,  $f_{0\Delta\Delta}^2/4\pi$ , used in the construction of the one-boson-exchange  $\Delta\text{N}$  potential and thereby it corresponds to different angular distributions<sup>(11)</sup>.

This indicates, as stressed before, that the collective resonance model results strongly depend on the model assumptions: for example on coupling constants, or on oscillator parameters, or on the size of the configuration space.

Despite the qualitative agreement found in the two cases now considered, in order to explain all the physical features of the excitation functions of differential cross sections, the influence of those uncertainties must be thoroughly investigated.

#### ACKNOWLEDGMENTS.

The authors are grateful to E. Bollini for the valuable contribution in the early stage of the analysis and to T. Bressani, F. Cannata, R. Mach, P. Quarati and M. G. Sapozhnikov for the helpful discussions.

REFERENCES.

- (1) - G. Giacomelli, P. Pini and S. Stagni, CERN-HERA, 69-1 (1969); F. J. Bussey, J. R. Carter, D. R. Dance, D. V. Bugg, A. A. Carter and A. M. Smith, Nuclear Phys. B58, 363 (1973).
- (2) - R. H. Landau, S. C. Phatak and F. Tabakin, Ann. Phys. 78, 299 (1973).
- (3) - N. D. Gabitzsch, G. S. Mutchler, C. R. Fletcher, E. V. Hungerford, L. Coulson, D. Mann, T. Witten, M. Furic, G. C. Phillips, B. Mayes, L. Y. Lee, J. Hudomalj, J. C. Allred and C. Goodmann, Phys. Letters 47B, 61 (1973); C. Wilkin, C. R. Cox, J. J. Domingo, K. Gabathuler, E. Pedroni, J. Rohlin, P. Schwaller and N. W. Tanner, Nuclear Phys. B62, 61 (1973); A. S. Clough, G. K. Turner, B. W. Allardyce, C. J. Batty, L. J. Baugh, W. J. McDonald, R. A. J. Riddle, L. M. Watson, M. E. Cage, G. J. Pyle and G. T. A. Squier, Nuclear Phys. B76, 15 (1974); A. S. Carrol, I. M. Chiang, C. B. Dover, T. F. Kycia, K. K. Li, P. O. Mazur, D. N. Michael, P. M. Mockett, D. C. Rahm and R. Rubinstein, Phys. Rev. 14C, 635 (1976).
- (4) - K. Bjornenak, J. Finjord, P. Osland and A. Reitan, Nuclear Phys. B22, 179 (1970); T. Kōh-mura, Nuclear Phys. B36, 228 (1972); C. Schmit, Lett. Nuovo Cimento 4, 454 (1970); L. A. Charlton and J. M. Eisenberg, Ann. Phys. 63, 286 (1971); W. R. Gibbs, Phys. Rev. C5, 755 (1972).
- (5) - C. Wilkin, Proceedings of Spring School on Pion Interactions at Low and Medium Energies, (SIN, CERN), CERN 71-14 (1971); C. Wilkin, Lett. Nuovo Cimento 4, 491 (1970).
- (6) - T. E. O. Ericson and J. Hüfner, Phys. Letters 33B, 601 (1970).
- (7) - M. P. Locher, O. Steinmann and N. Straumann, Nuclear Phys. B27, 598 (1971).
- (8) - J. E. Sedlak and W. A. Friedman, Phys. Rev. C16, 2306 (1977).
- (9) - F. Balestra, E. Bollini, L. Busso, R. Garfagnini, G. Piragino, A. Zanini, C. Guaraldo, R. Scrimaglio, I. V. Falomkin, M. M. Kulyukin, R. Mach, F. Nichitiu, G. B. Pontecorvo and Yu. A. Shcherbakov, Proceedings of the VII Intern. Conf. on Few Body Problems in Nuclear and Particle Physics (Delhi, 1976), p. 315; Torino-Dubna-Frascati Collaboration, Frascati report LNF-76/50 (1976).
- (10) - K. Klingenberg, M. Dillig and M. G. Huber, Preprint; E. Boschitz, Proceedings of the VII Intern. Conf. on High-Energy Physics and Nuclear Structure (Zürich, 1977), p. 133.
- (11) - R. Händel, M. Dillig and M. G. Huber, Phys. Letters 73B, 4 (1978).
- (12) - F. Balestra, L. Busso, R. Garfagnini, G. Piragino, R. Barbini, C. Guaraldo and R. Scrimaglio, Lett. Nuovo Cimento A12, 351 (1975) and A13, 673 (1975); F. Balestra, L. Busso, R. Garfagnini, G. Piragino, C. Guaraldo, A. Maggiora and R. Scrimaglio, Frascati report LNF-78/20 (1978).
- (13) - F. Balestra, L. Busso, R. Garfagnini, G. Piragino, R. Barbini, C. Guaraldo, R. Scrimaglio, I. V. Falomkin, M. M. Kulyukin and Yu. A. Shcherbakov, Nuclear Instr. and Meth. 119, 347 (1974) and 125, 157 (1975).
- (14) - F. Balestra, L. Busso, R. Garfagnini, G. Piragino, A. Zanini, C. Guaraldo, A. Maggiora and R. Scrimaglio, in press.
- (15) - Yu. A. Budagov, P. F. Ermolov, E. A. Kushnirenko, and V. I. Moskalev, Sov. Phys. -JEPT 15, 824 (1962); M. E. Nordberg and K. F. Kinsey, Phys. Letters 20, 692 (1966); K. M. Crowe, A. Fainberg, J. Miller and A. S. L. Parson, Phys. Rev. 180, 1349 (1969); R. Barbini, L. Busso, S. Costa, R. Garfagnini, C. Guaraldo, G. Piragino and R. Scrimaglio, Frascati report LNF-72/62 (1972); Yu. A. Shcherbakov, T. Angelescu, I. V. Falomkin, M. M. Kulyukin, V. I. Lyashenko, R. Mach, A. Mihul, N. M. Kao, F. Nichitiu, G. B. Pontecorvo, V. K. Sarycheva, M. G. Sapozhnikov, M. Semerdjeva, T. M. Troshev, N. I. Trosheva, F. Balestra, L. Busso, R. Garfagnini and G. Piragino, Nuovo Cimento A31, 249 (1976); F. Binon, P. Duteil, M. Gouarnère, L. Hugon, J. Jansen, J. P. Lagnaux, M. Palevsky, J. P. Peigneux, M. Spighel and J. P. Stroot, Nuclear Phys. A298, 499 (1978); I. V. Falomkin, V. I. Lyashenko, G. B. Pontecorvo, Yu. A. Shcherbakov, F. Balestra, R. Garfagnini, G. Piragino, T. Angelescu, A. Mihul and F. Nichitiu, Nuovo Cimento, 43A, 219 (1978).
- (16) - K. Roger and L. M. Lederman, Phys. Rev. 105, 250 (1957); A. M. Sachs, H. Winick and A. B. Wooten, Phys. Rev. 109, 1733 (1958); E. G. Pewitt, T. H. Fields, G. B. Yodh, J. G. Tetkovich and M. Derrick, Phys. Rev. 131, 1826 (1963); J. H. Norem, Nuclear Phys. B33, 512 (1971); K. Gabathuler, C. R. Cox, J. J. Domingo, J. Rohlin, N. W. Tanner and C. Wilkin, Nuclear Phys. B55, 397 (1973); R. H. Cole, J. S. McCarty, R. C. Minehart and E. A. Wadlinger, Phys. Rev. 17C, 681 (1978).

- (17) - Yu. A. Shcherbakov, T. Angelescu, I. V. Falomkin, M. M. Kulyukin, V. I. Lyashenko, R. Mach, A. Mihul, N. M. Kao; F. Nichitiu, G. B. Pontecorvo, V. K. Sarycheva, M. G. Sapozhnikov, M. Semerdjeva, T. M. Troshev, N. I. Trosheva, F. Balestra, L. Busso, R. Garfagnini and G. Piragino, *Nuovo Cimento* A31, 262 (1976); I. V. Falomkin, V. I. Lyashenko, G. B. Pontecorvo, Yu. A. Shcherbakov, F. Balestra, R. Garfagnini, G. Piragino, T. Angelescu, A. Mihul and F. Nichitiu, *Nuovo Cimento* 43A, 219 (1978).
- (18) - H. Byfield, J. Kessler and L. M. Lederman, *Phys. Rev.* 86, 17 (1952); W. F. Baker, M. Byfield and J. Rainwater, *Phys. Rev.* 112, 1773 (1958); R. M. Edelstein, W. F. Baker and J. Rainwater, *Phys. Rev.* 122, 252 (1961); F. Binon, P. Duteil, J. P. Garron, J. Gorres, L. Hugon, J. P. Peigneux, C. Schmit, M. Spighel and J. P. Stroot, *Nuclear Phys.* B17, 168 (1970); H. Dollard, K. L. Erdman, R. R. Johnston, T. Masterson and P. Walden, *Phys. Letters* B63, 416 (1976); J. Piffaretti, R. Corfù, J. P. Egger, P. Gretilat, C. Lunke, C. Perrin and E. Schwarz, *Phys. Letters* B67, 289 (1977); S. A. Dytman, J. F. Amann, P. D. Barnes, J. N. Craig, K. G. R. Doss, R. A. Eisestein, J. D. Sherman, W. R. Whatson, R. J. Peterson, G. R. Burlerson, S. L. Verbeck and H. A. Thiessen, *Phys. Rev.* 38, 1059 (1977).
- (19) - D. J. Malbrough, C. W. Darden, R. D. Edge, T. Marks, B. M. Preedom, R. L. Burman, M. A. Moinester, R. P. Redwine, F. E. Bertrand, J. P. Cleary, E. E. Gross, C. A. Ludeman and K. Gotow, *Phys. Rev.* 17C, 1395 (1978); J. P. Albanese, J. Arvieux, E. Boschitz, C. H. Q. Ingram, L. Pflug, C. Wiender and J. Zichy, *Phys. Letters* 73B, 119 (1978).
- (20) - L. S. Kisslinger and W. L. Wang, *Phys. Rev. Letters* 30, 1071 (1973); L. S. Kisslinger and W. L. Wang, *Ann. Phys. (N. Y.)* 99, 374 (1976).
- (21) - M. Dillig and M. G. Huber, *Phys. Letters* 48B, 417 (1974); M. Dillig and M. G. Huber, in: *Mesonic Effects in Nuclear Structure*, ed. by K. Bleuer et al. (Bibl. Institut., Mannheim, 1975), p. 80; M. Dillig and M. G. Huber, in: *Interaction Studies in Nuclei*, ed. by H. Jochim and B. Ziegler (North-Holland Publ. Co., 1975), p. 781.
- (22) - F. Lenz, *Ann. Phys. (N. Y.)* 95, 348 (1975); F. Lenz and E. J. Moniz, *Phys. Rev.* C12, 909 (1975); F. Lenz, in: *Proceedings of the Intern. Conf. on Meson-Nuclear Physics*, ed. by P. D. Barnes et al. (Carnegie-Mellon, 1976), p. 403; M. Hirata, F. Lenz and K. Yazaki, SIN preprint (1976); M. Hirata, J. H. Koch, F. Lenz and E. J. Moniz, Preprint (1977).
- (23) - G. E. Brown and W. Weise, *Phys. Reports* 22, 909 (1975); W. Weise, *Nuclear Phys.* A278, 402 (1977).